Anal Bioanal Chem (2008) 392:717–726
DOI 10.1007/s00216-008-2308-1

ORIGINAL PAPER

Direct and simultaneous profiling of epoxyeicosatrienoic acid enantiomers by capillary tandem column chiral-phase liquid chromatography with dual online photodiode array and tandem mass spectrometric detection

Ladislau Kiss · Jens Bier · Yasmin Röder · Norbert Weissmann · Friedrich Grimminger · Werner Seeger

Received: 18 January 2008 / Revised: 7 July 2008 / Accepted: 18 July 2008 / Published online: 19 August 2008

Abstract Despite first evidence for the cytochrome P450-mediated enantioselective biosynthesis and activity of *cis*-epoxyeicosatrienoic acids (EETs), as yet little is known about the stereospecifity of EET generation and physiology, because the existing chiral methods are time consuming, labor intensive, and not sensitive enough. We present a method for highly sensitive, direct, *and* simultaneous chiral analysis of all eight EET enantiomers consisting of (i) solid-phase extraction, (ii) reversed-phase high-performance liquid chromatographic purification followed by (iii) consecutive regio- and enantiomeric separation of the four *underivatized* EET regioisomers within *one* chromatographic run employing capillary tandem column chiral-phase liquid chromatography with (iv) reliable dual online photodiode array and gentle electrospray ionization tandem mass spectrometric identification and quantitation of the eluting optical antipodes. This one-step, simple, expeditious, and highly sensitive measurement allows profiling of all eight EET enantiomers at once, thus avoiding substance loss and enabling high sample throughput. Limits of quantification in the low picogram range were achieved by the use of capillary columns with typical high quantitative sensitivity instead of conventional columns with low chromatographic signal intensity employed by previous methods. Application to tissue homogenates demonstrated the suitability of this approach for routine and reliable "enantioprofiling" of *free* endogenous EETs, i.e., EETs not esterified into cellular membrane phospholipids, typically occurring at very low concentrations. The technique can readily be employed for preparative purification of enantiomers in the microgram range using large-inner-diameter columns.

Keywords Profiling of epoxyeicosatrienoic acid enantiomers · Capillary tandem column chiral-phase liquid chromatography · Photodiode array detection · Electrospray ionization tandem mass spectrometry · Multiple reaction monitoring · Extracted ion chromatogram

Abbreviations

CYP	cytochrome P450
AA	arachidonic acid
EET	epoxyeicosatrienoic acid
EETE	epoxyeicosatetraenoic acid
EPA	eicosapentaenoic acid
IS	internal standard
BHT	butylated hydroxytoluene
EDHF	endothelium-derived hyperpolarizing factor
SPE	solid-phase extraction
HPLC	high-performance liquid chromatography
CapLC	capillary liquid chromatography
CP	chiral-phase
RP	reversed-phase

Electronic supplementary material The online version of this article (doi:10.1007/s00216-008-2308-1) contains supplementary material, which is available to authorized users.

L. Kiss (✉) · J. Bier · Y. Röder · N. Weissmann · F. Grimminger · W. Seeger
Biochemie Med. II, University of Gießen Lung Center (UGLC), Department of Internal Medicine, Justus Liebig University, Paul Meimberg Str. 5, 35392 Gießen, Germany
e-mail: ladislau.kiss@innere.med.uni-giessen.de

ODS	octadecyl silyl
RT	retention time
RRI	relative retention index
PDA(D)	photodiode array (detector/detection)
ESI	electrospray ionization
MS	mass spectrum/spectrometric/spectrometer/ spectrometry
CapTC-CP-LC-PDAD-ESI-MS^2	capillary tandem column chiral-phase liquid chromatography with dual photodiode array and electrospray ionization tandem mass spectrometric detection
MRM	multiple reaction monitoring
CT	column temperature
L	length
i.d.	inner diameter
LOQ	limit of quantitation
KHB	Krebs–Henseleit buffer
DEA	diethylamine
TEA	triethylamine
FA	formic acid
AcOH	acetic acid
iPA	isopropyl alcohol
EtOH	ethanol
nHex	*n*-hexane
EDTA	ethylenediaminetetraacetic acid

Introduction

Cytochrome P450 (CYP) monooxygenases metabolize arachidonic acid (AA) to four regioisomeric *cis*-epoxyeicosatrienoic acids (EETs)—14,15-, 11,12-, 8,9-, and 5,6-EET—each consisting of a pair of enantiomers: 14(*R*),15(*S*)-/14(*S*),15(*R*)-EET, 11(*R*),12(*S*)-/11(*S*),12(*R*)-EET, 8(*R*),9(*S*)-/8(*S*),9(*R*)-EET, and 5(*R*),6(*S*)-/5(*S*),6(*R*)-EET, respectively [1] (Fig. 1). EETs are generated in all tissues [1, 2], sometimes representing the dominant eicosanoid group [3], and display a broad array of biological actions including

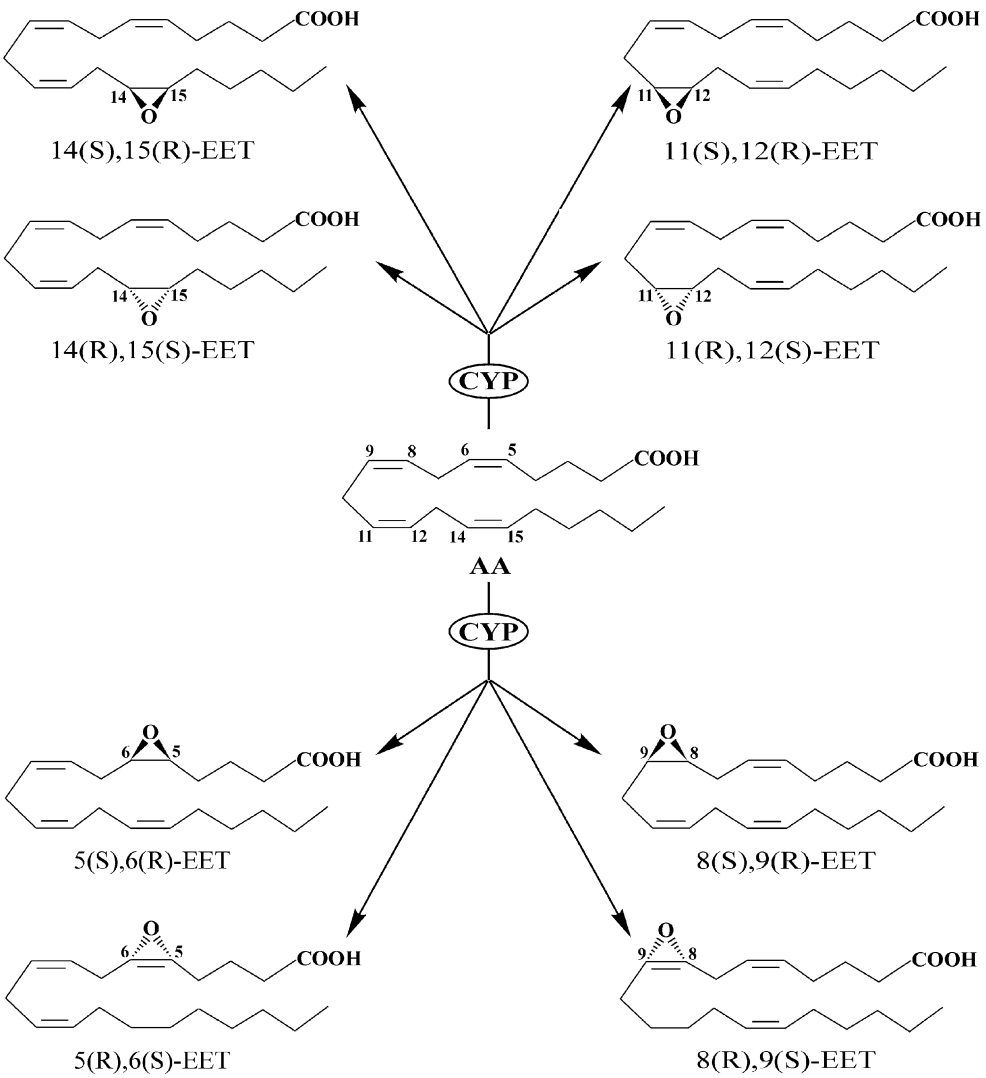

Fig. 1 Formation of EET enantiomers from AA via CYP epoxygenase

modulation of electrolyte transport processes [1, 4], potentiation of vascular cell proliferation [5], inhibition of platelet aggregation [1, 6, 7] and vascular cell migration [8], and partially opposite vasoregulative activities from vasodilatation to vasoconstriction [1, 2, 9–14]. In the last decade EETs gained particular interest as putative chemical correlates of the vasodilatative endothelium-derived hyperpolarizing factor (EDHF) in the coronary vasculature [15–17] stimulating proliferation of vascular cells [18] and as anti-inflammatory agents preventing leukocyte adhesion to the vascular wall [19]. EETs are generated stereospecifically by various CYP isoforms from many sources (e.g., 1A1, 1A2, 2A1, 2B1, 2B2, 2C11, 2C12 from rat liver; 2C8, 2C9 from human liver; 2B4 from rabbit lung) [1, 20–27] and their actions are elicited by specific optical isomers: 14(*R*),15(*S*)-EET is a stereospecific inhibitor of cyclooxygenase [6], 11(*R*),12(*S*)-EET is a potent renal vasodilator [28], and 8(*S*),9(*R*)-EET is a renal vasoconstrictor [24], whereas their optical antipodes, 14(*S*),15(*R*)-EET, 11(*S*),12(*R*)-EET, and 8(*R*),9(*S*)-EET, respectively, are inactive.

Despite the multitude of contradictory reports on the physiological actions of EETs and clear evidence for both stereospecific biosynthesis and activity, in most studies they are not assessed by chiral analysis, meaning that no correlation between the occurrence of a specific enantiomer and its putative biological action was possible. Consequently, inconsistent findings regarding the physiology of EETs, as, e.g., the longtime controversy about their putative role as EDHF, might be elucidated by correlating the physiological function with the generation of stereoisomers, rather than with that of regioisomers. The lack of chiral EET analysis is obviously a result of the fact that previous methods are extremely labor intensive and/or time consuming and not sensitive enough. These techniques comprise multistep procedures susceptible to substance loss, like low-yield derivatization prior to *individual* chiral resolution and quantitation [29, 30] or direct, i.e., without previous derivatization, but likewise *individual* separation of each regioisomer into the corresponding pair of enantiomers either with a different mobile phase [31, 32] or with the same mobile phase at different flow rates [32] instead of direct *and* simultaneous chiral resolution of *all* eight enantiomers within *one* chromatographic run. Additional proneness to loss of the thermolabile EETs results from the use of high-temperature detection modes. In all cases, quantitative sensitivity is dramatically reduced by the use of large-inner-diameter (4.6 mm) conventional chiral columns with low chromatographic signal intensity instead of capillary columns (i.d.<500 μm) with typical high quantitative sensitivity. Accordingly, there was compelling rationale to develop a time-saving, direct, simple one-step *and* highly sensitive capillary chiral analysis as a tool to facilitate and improve work in this area by enabling routine systematic *and* sensitive assessment of the distribution of *free* EET antipodes as a prerequisite for new insights into the biological functions of EET enantiomers.

We present a method comprising (i) solid-phase extraction (SPE), (ii) reversed-phase (RP) HPLC purification, (iii) highly sensitive *capillary* tandem column chiral-phase liquid chromatographic (CapTC-CP-LC) nonoverlapping separation of *all* eight *underivatized* EET enantiomers within *one* run using a setup of two serially coupled columns followed by both online (iv) photodiode array (PDA) and *gentle* electrospray ionization (ESI) *tandem* mass spectrometric (MS^2) detection in the negative ion mode for identification and quantitation of eluting analytes in the low picogram range. Application of this one-step CapTC-CP-LC-PDAD-ESI-MS^2 technique of high quantitative sensitivity (owing to the use of capillary columns) to complex biological material like lung and kidney homogenate demonstrated the robustness, reliability, and sensitivity of this method in routine high-sample-throughput profiling of endogenous *free* EET enantiomers ("enantioprofiling"), i.e., EETs not esterified into cellular membrane phospholipids, typically occurring at very low concentrations in biological sources. The method can flexibly be used for efficient preparative purification of EET enantiomers in the microgram range with large-i.d. columns.

Experimental

Standards, reagents, and solvents

The racemates (±)14,15-, (±)11,12-, (±)8,9-, and (±)5,6-EET were from Biomol (Hamburg, Germany), Cayman Chemical Company (Ann Arbor, USA), and Cascade Biochem (Reading, UK). The stereoisomers 14(*R*),15(*S*)-/14(*S*),15(*R*)-EET, 11(*R*),12(*S*)-/11(*S*),12(*R*)-EET, 8(*R*),9(*S*)-/8(*S*),9(*R*)-EET, 5(R),6(S)-/5(*S*),6-(R)EET were from Cascade and WAK Chemie (Bad Homburg, Germany). The antipodes 14(*R*),15(*S*)-/14(*S*),15(*R*)-EET were also from Sigma (Munich, Germany). The deuterated standards [$^2H_8$]14,15-, [$^2H_8$]11,12-, [$^2H_8$]8,9-EET, and [$^2H_8$]5,6-EET-Me and the internal standard (IS) eicosapentaenoic acid (EPA) were from Biomol. (±)14,15-Epoxy-5*Z*,8*Z*,11*Z*,17*Z*-eicosatetraenoic acid (designated throughout this study simply as EETE) was from Cayman. EET standards and EPA were checked for purity and concentration as described elsewhere [33, 34]. The antioxidant butylated hydroxytoluene (BHT), triethylamine (TEA), diethylamine (DEA), acetic acid (AcOH), and formic acid (FA) were from Sigma. Ethylenediaminetetraacetic acid tetrasodium salt, tetrahydrate (EDTA $Na_4{\cdot}4H_2O$) was from E. Merck (Darmstadt, Germany). Krebs–Henseleit buffer supplemented with 5% hydroxyethyl starch (KHB) was

from Serag Wiessner (Naila, Germany). Water was purified with a Milli-Q system (Millipore, Eschborn, Germany). Methanol was from Burdick & Jackson (Muskegon, MI, USA), acetonitrile was from J.T. Baker (Deventer, Netherlands), and isopropyl alcohol (iPA) was from Fluka AG (Buchs, Switzerland). Ethanol (EtOH) and *n*-hexane (nHex) were from Riedel-de Haën (Seelze, Germany). The solvent mixtures used for SPE are listed in the Electronic Supplementary Material (Table S1).

Analytical procedures and equipment

Sample extraction

Cleanup and concentration were performed by multistep SPE as displayed in the Electronic Supplementary Material (Table S2). For the assessment of recoveries (quality controls) we used tissue homogenate (lung and kidney from rabbit and rat) as biological sample matrix and KHB as EET-free sample matrix. Aliquots (2 ml each) of KHB in homogenizer tubes were supplemented with 60 μl FA, 56 μl BHT 1% in methanol, 40 μl of solution E (Electronic Supplementary Material Table S1) and spiked with mixtures of known amounts of enantiomerically pure EET standards and BHT. Constant amounts of deuterated EETs and/or EPA as IS were added. Alternatively, whole blood-free rinsed rabbit/rat lungs or blood- and urine-free rinsed rabbit/rat kidneys were quickly cut into small pieces. Minced tissue samples (2 g each) were placed into 5-ml chilled homogenizer borosilicate glass tubes, each containing 60 μl FA, 56 μl BHT 1% in methanol, 40 μl of solution E, known amounts of enantiomerically pure EET standards, and constant amounts of deuterated EETs and/or EPA as IS and subjected to mechanical homogenization for 10 min at 1,500 rpm employing a Potter S homogenizer with PTFE plunger mounted on a stainless steel shaft, all from Sartorius AG (Göttingen, Germany). Genuine biological samples (for assessment of endogenous enantiomers from tissue homogenate) were processed in the same manner, except for supplementation with EET standards.

Homogenates (2 g each of quality controls or genuine samples) and 2-ml aliquots of KHB were supplemented with 0.8 ml of solvent mixture F, vortexed, and the contents were transferred to 10-ml glass tubes. Homogenizer tubes were rinsed with 2 ml of solvent mixture F, and the contents were combined with the original sample. The diluted homogenate samples were vortexed for 10 min and centrifuged for 60 min at 4,460×*g* and 4 °C.

Prior to SPE, 2.4 ml of supernatant was diluted with 17.6 ml of ice-cold KHB and applied to the conditioned extraction cartridges filled with end-capped octadecyl silyl (ODS) silica (Chromabond; C18 ec, 200 mg sorbent) mounted in a vacuum manifold, all from Macherey-Nagel (Düren, Germany). After the final elution step, the collected samples were dried gently under a stream of N_2 and subjected to purification by a modified version of a previous RP-HPLC procedure (see "EET purification by RP-HPLC" in the Electronic Supplementary Material).

TC-CP-LC-PDAD-ESI-MS^2 procedures and instrumentation

Stereoisomers were separated with a setup consisting of two consecutively connected columns: an amino column (Grom-Sil 300 Amino-4PR, *L*=60 mm, particle size 3 μm) followed by a chiral column (Chiralcel OD-H, *L*=250 mm; filled with cellulose tris(3,5-dimethylphenyl carbamate) on a 5-μm silicagel substrate). The following column sizes were used:

(a) Capillary columns (i.d.=300 μm or 150 μm) for CapCP-LC analysis, and
(b) Large-i.d. columns, i.e., narrowbore columns (i.d.= 2.0 mm) or conventional columns (i.d.=4.6 mm) for preparative chiral purification of enantiomers.

All amino columns and the capillary/narrowbore chiral columns were from Grom Analytik + HPLC (Rottenburg-Hailfingen, Germany). The conventional chiral columns were from Daicel Chemical Industries, Niigata, Japan, and Chiral Technologies Europe, Illkirch, France. The same mobile phase consisting of 99.7:0.21:0.09:0.015 (v/v/v/v) nHex, iPA, EtOH, and AcOH was used with all column sizes. Flow rates were 2.8 μl/min, 8 μl/min, 380 μl/min, and 1.8 ml/min with 150-μm-i.d., 300-μm-i.d., 2-mm-i.d., and 4.6-mm-i.d. columns, respectively.

The instrumental setup used for chiral analysis consisted of two main parts: (i) a 1100 Series capillary LC unit (Agilent Technologies Deutschland, Waldbronn, Germany) interfaced with (ii) an Esquire 3000+ ion trap mass spectrometer (Bruker Daltonik, Bremen, Germany).

(i) The CapLC unit consisted of a micro autosampler, a fraction collector, a micro pump, and a photodiode array detector (PDAD). This setup could readily be adapted to (a) CapCP-LC analysis employing capillary columns and to (b) preparative HPLC conditions employing large-i.d. columns, as follows:
    (a) For CapTC-CP-LC-PDAD-ESI-MS^2, the autosampler and PDAD were equipped with an 8-μl sample loop and a nano flow cell (500-nl volume, 10-mm path length), respectively.
    (b) For preparative chiral purification of deuterated and nondeuterated EET enantiomers, autosampler and PDAD were equipped with a 40-μl sample loop and an analytical flow cell (10-μl volume, 10-mm path length), respectively.

(ii) The ionization process of analytes necessary for ESI-MS^2 detection was assisted, as described elsewhere [35–37], by post-column mixing of the nonpolar water-free LC effluent with a polar makeup solution consisting of a 50:34:16 (v/v/v) mixture of iPA, DEA, and AcOH prior to reaching the ESI source. The makeup solution was infused into the LC effluent of the 300-μm-i.d. capillary columns at a flow rate of 10 μl/h via a tee connector integrated into the fused-silica connecting tubing between PDAD and MS using a syringe pump (Cole-Parmer Instrument Company, Vernon Hills, IL, USA).

N_2 was used as nebulizing and drying gas, and He was used as collision gas. Nebulizing gas pressure, drying gas flow, and drying gas temperature were set to 12.0 psi, 6.0 l/min, and 200 °C, respectively. Capillary voltage, collision energy in terms of fragmentation amplitude, isolation width, and mass cutoff were set to 2,800–3,200 V, 0.58–0.67 V, 1.5–2.0 Da, and *m/z* 85, respectively.

Prior to injection of 8-μl aliquots into the CapTC-CP-LC-PDAD-ESI-MS^2 system, biological or quality control samples dried after RP-HPLC purification were redissolved in 40 μl of pure hexane or mobile phase containing 30 μM BHT. Calibration standard mixtures were redissolved and diluted with the same solvents, and supplemented with constant amounts of IS and EETE. The eluting enantiomers were subjected to dual online spectrophotometric and tandem mass spectrometric analysis employing the consecutively interfaced PDAD and ion trap. PDAD provided full UV spectra (190 to 400 nm) of eluting analytes and allowed checking for peak purity and subtraction of possible coeluting material. The ion trap was operated in the negative ion mode employing multiple reaction monitoring (MRM) for the simultaneous acquisition of MS^2 spectra and traces of coeluting nonisomeric analyte precursor ions.

The relative retention index (RRI) for chiral chromatographic characterization of EET enantiomers by comparison of their retention times (RT) to those of the reference substances EPA and EETE was calculated by the following equation:

$$\mathrm{RRI} = \frac{\mathrm{RT(analyte)} - \mathrm{RT(EPA)}}{\mathrm{RT(EETE)} - \mathrm{RT(EPA)}}$$

The elution order of EET enantiomers was assigned by comparison with the chromatographic properties of enantiomerically pure commercial standards as well as enantiomers prepared from commercial racemic standards using the method of Zhang and Blair [31] and/or the preparative version of the present approach.

Thus, triple analyte identification was performed: chromatographically by RRI, and by both UV and MS^2 spectra of the peaks detected on the optical and MS^2 traces, respectively.

Quantitation was performed by IS method using standard mixtures which contained:

(i) EPA as a *common* IS when UV *and* MS^2 or UV detection *alone* was employed, or
(ii) Deuterated EET standards *and* EPA as IS when MS^2 detection *alone* was used.

Biological matrix

The distribution of *free* EET enantiomers was assessed in tissue homogenate from hypoxic lungs as well as from control lungs and kidneys of rabbits and rats (see "Physiological experiments" in the Electronic Supplementary Material).

Results and discussion

Direct and simultaneous CapTC-CP-LC-PDAD analysis

The presented chiral separation technique was developed by starting with the chiral chromatographic conditions described by Zhang and Blair [31] for underivatized EETs, i.e., use of a conventional (4.6-mm i.d.) Chiralcel OD column and resolution of each pair of enantiomers with a separate mobile phase consisting of different proportions of nHex, iPA, and AcOH.

The concept of *one-step* chiral analysis was to obtain *direct* (i.e., without EET derivatization), *simultaneous*, and *highly sensitive* CapTC-CP-LC separation of all four regioisomers into the corresponding pairs of enantiomers without peak overlapping in *one* chromatographic run followed by *online*, i.e., direct and thus sensitive tandem ESI-MS^2 identification and quantitation of the eluting antipodes. Direct *and* simultaneous nonoverlapping chiral resolution within one run was a result of column choice and setup, development of an appropriate mobile phase, and use of optimal column temperature (CT) as detailed in "Method development strategy" in the Electronic Supplementary Material. Optimization trials were performed with a standard mixture consisting of the four racemic EET regioisomers, EPA, and EETE. Eluting compounds were monitored at 204 nm. Ultimately, injection of the standard mixture on the tandem column setup—nonchiral followed by chiral column—resulted in both regioisomeric *and* enantiomeric separation, i.e., simultaneous *and* consecutive resolution of all four pairs of enantiomers within one chromatographic run without diastereoisomeric peak overlapping (Fig. 2a).

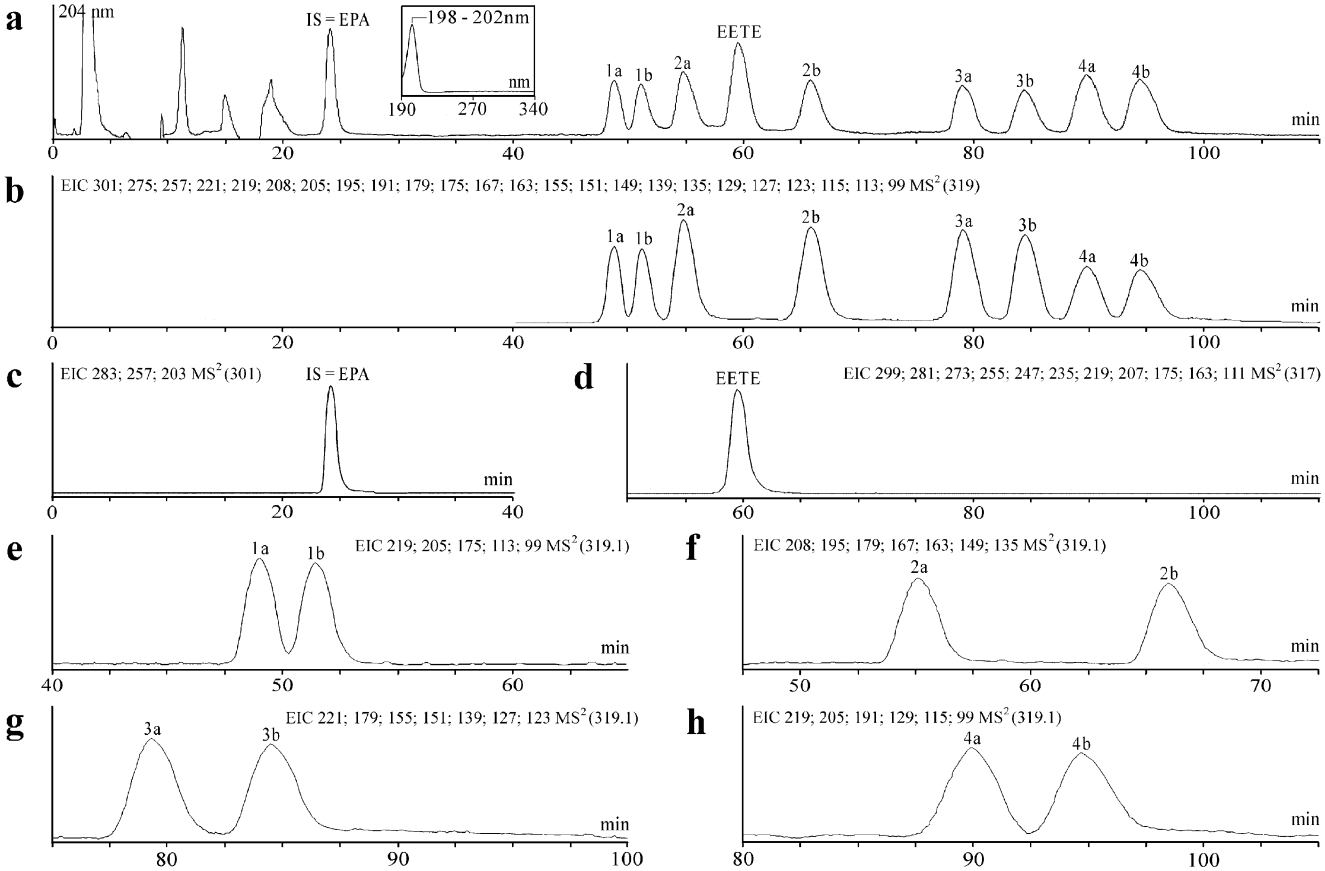

Fig. 2 Simultaneous separation of the four racemic underivatized EET regioisomers into the corresponding consecutively eluting nonoverlapping pairs of enantiomers in *one* chromatographic run as a result of tandem capillary (i.d.=0.300 mm) column coupling [a nonchiral Grom-Sil Amino-4PR column for effective regioisomeric separation followed by a Chiralcel OD-H chiral column for simultaneous enantiomeric resolution, both with CT set to 26 °C] and isocratic normal-phase elution using a 99.7:0.21:0.09:0.015 (v/v/v/v) mixture of nHex, iPA, EtOH, and AcOH as mobile phase at a flow rate of 8 μl/min. An 8-μl aliquot of a mixture consisting of the four racemic regioisomeric EET standards, EPA as an IS and a reference substance for RRI calculation, and EETE as a second reference substance for RRI calculation were injected into the CapTC-CP-LC-PDAD-ESI-MS^2 system. Online PDAD enabled monitoring of CapTC-CP-LC-PDAD chromatograms at 204 nm and identification of eluting analytes by online spectra plot on the peak apex (see *inset*) as well as peak purity control-assisted quantitation (**a**). Serial interfacing of the PDAD with an ESI ion trap mass spectrometer enabled online monitoring of CapTC-CP-LC-ESI-MS^2 chromatograms of the eluting compounds in the negative ion mode employing MRM. MS^2 analysis was performed by identification and quantitation of substance peaks on the EIC MS^2 traces defined for the precursor anions at *m/z* 319 (EET enantiomers) (**b**, **e**, **f**, **g**, and **h**), 301 (EPA) (**c**), and 317 (EETE) (**d**). The regiospecific EIC MS^2 trace definitions of the neighboring pairs of enantiomers 14(*S*),15(*R*)-EET/14(*R*),15(*S*)-EET (**e**) and 11(*S*),12(*R*)-EET/11(*R*),12(*S*)-EET (**f**) as well as 8(*R*),9(*S*)-EET/ 8(*S*),9(*R*)-EET (**g**) and 5(*R*),6(*S*)-EET/5(*S*),6(*R*)-EET (**h**), respectively, contained no common fragments, thus enabling accurate assessment of the enantiomeric ratios even under conditions of coelution between the regioisomeric pairs 14,15-EET and 11,12-EET as well as 8,9-EET and 5,6-EET, respectively, e.g., due to aging-dependent alteration of the amino column. The nonregiospecific definition of the EIC MS^2 trace in **b** included all signals from the regiospecific EIC MS^2 trace definitions in panels **e**, **f**, **g**, and **h**. Peak designation: *1*=(±)14,15-EET; *1a*=14(*S*),15(*R*)-EET; *1b*=14(*R*),15(*S*)-EET; *2*=(±)11,12-EET; *2a*=11(*S*),12(*R*)-EET; *2b*=11(*R*),12(*S*)-EET; *3*=(±)8,9-EET; *3a*=8(*R*),9(*S*)-EET; *3b*=8(*S*),9(*R*)-EET; *4*=(±)5,6-EET; *4a*=5(*R*),6(*S*)-EET; *4b*=5(*S*),6(*R*)-EET; *IS* = EPA; EETE

CapTC-CP-LC-ESI-MS^2 analysis

The molecular carboxylate ions of the EETs, EETE, and EPA (designated *a*) yielded noncharacteristic fragments due to neutral loss of CO_2 (*b* = *a*−CO_2), H_2O (*a*−H_2O), CO_2 *and* H_2O (*b*−H_2O), and characteristic fragments due to the position of the epoxide function and double bonds (Table S3). The MS^2 spectra are shown in Electronic Supplementary Material Fig. S3 with the characteristic fragments designated *c*, *d*, *e*, *f* etc. The online MS^2 spectra obtained by fragmentation of the molecular ions of the EETs (*a* at *m/z* 319) under normal-phase conditions were similar to those generated under reversed-phase conditions [34, 38–42].

The MS raw data acquired with the online interfaced ion trap operated in the negative ion mode using MRM were used, as described elsewhere [38, 39], for the definition of extracted ion chromatograms (EIC MS^2) of the eluting analytes by summing the intensities of substance-specific signals from the

MS^2 spectra of the precursor ions (Fig. 2b–d). Moreover, regiospecific EIC MS^2 trace definitions (Fig. 2e–h) enabled chiral analysis even under conditions of overlapping diastereoisomeric peaks, i.e., when the regioisomers 14,15- and 11,12-EET or/and 8,9- and 5,6-EET are poorly resolved. These EIC MS^2 trace definitions contain a restricted selection of regioisomer-specific signals, so that the traces of the neighboring regioisomers 14,15-EET and 11,12-EET (EIC 219; 205; 175; 113; 99 MS^2 (319) and EIC 208; 195; 179; 167; 163; 149; 135 MS^2 (319), respectively), and those of 8,9-EET and 5,6-EET (EIC 221; 179; 155; 151; 139; 127; 123 MS^2 (319) and EIC 219; 205; 191; 129; 115; 99 MS^2 (319), respectively) do not share common signals. Thus, the present tandem-mass-spectrometry-based technique enabled individual identification and quantitation of each regioisomer by substance-specific EIC MS^2 traces, regardless of isomeric matrix interferences.

Preparative purification of EET enantiomers

Preparative purification of optical isomers in the microgram range from commercial racemates was performed with the same mobile phase as for CapCP-LC and the corresponding setup of large-i.d. columns, as specified in the Experimental. Chromatographic selectivity and the influence of CT on chiral resolution was similar under capillary, narrowbore, and conventional LC conditions. Thus, the UV chromatograms obtained with large-i.d. columns (not shown) corresponding to the three separation modes described in "Method development strategy" in the Electronic Supplementary Material, i.e.,

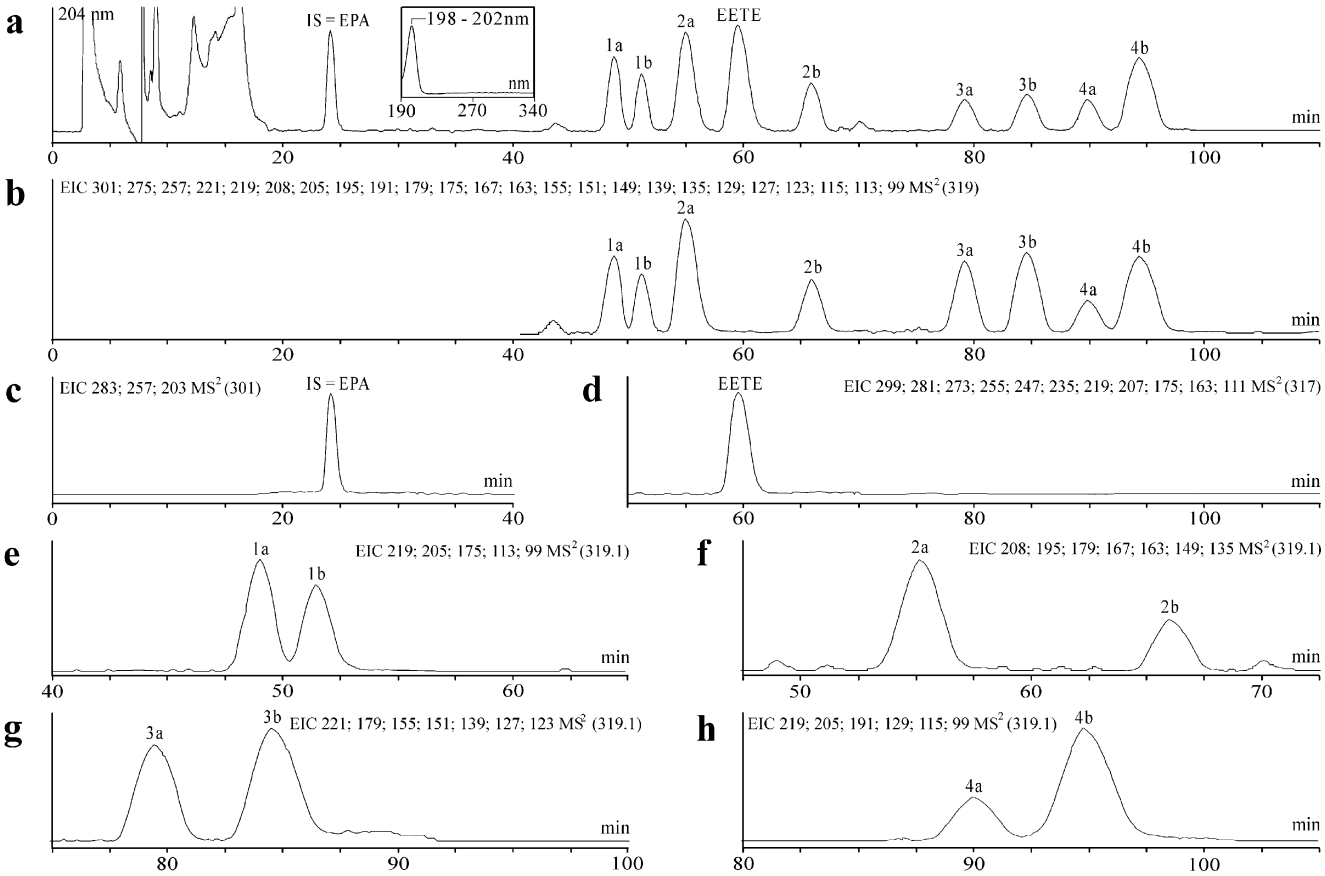

Fig. 3 Chromatographic profiles of EET enantiomers from hypoxic rabbit lung homogenate obtained by CapTC-CP-LC-PDAD-ESI-MS^2. Homogenate samples were subjected to SPE followed by RP-HPLC purification and finally analyzed by isocratic one-step CapTC-CP-LC-PDAD-ESI-MS^2 as described in Fig. 2. Eluting compounds were assessed by integration of the peaks detected at 204 nm by online PDAD (**a**) with analyte identification by spectra plot on the peak maximum (*inset* in panel **a**) and subsequent tandem MS^2 detection with the online interfaced ion trap in the negative ion mode employing MRM. Integration and MS^2 analysis of substance peaks were performed on the EIC MS^2 traces defined for the precursor anions at *m/z* 319 (EETs), 301 (EPA), and 317 (EETE) (**b**, **c**, and **d**, respectively), as well as on the regiospecific EIC MS^2 traces defined for the peak pairs 14(*S*),15(*R*)-EET/14(*R*),15(*S*)-EET (**e**), 11(*S*),12(*R*)-EET/11(*R*),12(*S*)-EET (**f**), 8(*R*),9(*S*)-EET/8(*S*),9(*R*)-EET (**g**), and 5(*R*),6(*S*)-EET/5(*S*),6(*R*)-EET (**h**) (see also Fig. 2e–h). For assessment of the enantiomeric ratios, the data obtained by peak integration on both the nonregiospecific EIC MS^2 trace defined for all EET regioisomers (**b**) as well as on the regiospecific EIC MS^2 trace definitions (**e**, **f**, **g**, **h**) were employed. Owing to optimal regioisomeric separation, the results obtained with these two types of EIC MS^2 trace definitions were virtually identical. Peak designation is the same as in Fig. 2

(i) CT=26 °C, (ii) CT=4 °C, and (iii) CT=36 °C, were similar to the CapCP-LC traces in Electronic Supplementary Material Figs. S2c, d, and e, respectively. Consequently, for purification with maximal recovery of the 14,15-, 11,12-EET, and EETE enantiomers, mode (ii) at CT=4 °C was used. The second EETE antipode was used as reference substance for chiral chromatographic RRI calculation. Mode (iii) at CT=36 °C was used for efficient purification of the 8,9- and 5,6-EET antipodes.

Assessments of calibration and recovery

Calibration of UV and MS signal performed by IS method, employing EPA as a common IS for all analytes, yielded linear regression functions (R^2>0.998) for all EET stereoisomers (exemplified for MS^2 signal calibration in Electronic Supplementary Material Fig. S4).

SPE followed by RP-HPLC purification and CapTC-CP-LC-PDAD-ESI-MS^2 was applied to biological samples and to EET-free KHB, both spiked with known amounts of nondeuterated enantiomerically pure standards, and deuterated enantiomers and/or EPA as IS (see the Experimental), yielding linear plots and recoveries >70% for all EETs (Electronic Supplementary Material Table S4). Comparison of recoveries obtained by adding constant amounts of EPA *and* deuterated EETs as IS before SPE, prior to any manipulation, to both the biological matrix and KHB, showed no significant differences (<RSD_{max}=9%), demonstrating that EPA and deuterated EETs were equally suitable for serving as the IS. Moreover, the ratios between the recovery of EPA and the recoveries of all enantiomers remained unchanged during sample preparation. Thus, we decided on the more convenient use of EPA as an IS for both MS^2 and PDA detection and, together with EETE, as a reference substance for the calculation of the chiral RRI.

With 300-μm-i.d. columns, the limits of quantitation (LOQ) for MS^2 detection of EET enantiomers, defined as the on-column analyte amount at a signal to noise (S/N) ratio >12, were 30 pg, 30 pg, 40 pg, and 60 pg for the 14,15-, 11,12-, 8,9-, and 5,6-enantiomers, respectively. With 150-μm-i.d. columns, the LOQ for MS^2 detection were four times lower. Overall, the LOQ for PDAD were higher than MS^2 detection results by a factor of 30. RSD<9%, n=6.

The actual recoveries were checked with quality control samples freshly prepared prior to SPE of a sample batch as specified in "Quality control samples" in the Electronic Supplementary Material.

Characteristics of CapTC-CP-LC-PDAD-ESI-MS^2 analysis

Although separation of EET enantiomers with Chiralcel columns goes back to the end of the 1980s [29] and has successfully been used for elucidation of the stereoselective biosynthesis and physiology of EETs [6, 12, 21–28], these methods have a series of disadvantages with two main detrimental consequences—(a) very long overall analysis time and (b) low quantitative sensitivity—rendering them unpractical for sensitive and reliable routine chiral analysis with high sample throughput.

The inherent disadvantages of previous methods employing *individual conventional* CP-HPLC separation of each enantiomer were overcome by the present tandem column *one-step* chiral analysis, which provides the highest quantitative sensitivity owing to the use of *capillary* columns, and displays the following main advantages:

(1) High sample throughput compared with previous chiral methods for profiling of EET enantiomers, thus enabling routine analysis,
(2) LOQ in the low picogram range, and

Table 1 Profiling of *free* EET enantiomers ("enantioprofiling") generated in rabbit and rat lung and kidney

EET regioisomer	Enantiomeric ratio (%)									
	HRbL[a]		CRbL[b]		CRaL[c]		CRbK[d]		CRaK[e]	
	S,R	*R,S*	*S,R*	*R,S*	*S,R*	*R,S*	*S,R*	*R,S*	*S,R*	*R,S*
14,15-EET	60*	40*	46	54	38*	62*	49	51	58	42
11,12-EET	71*	29*	76*	24*	39*	61*	83*	17*	52	48
8,9-EET	55	45	60*	40*	63*	37*	22*	78*	35*	65*
5,6-EET	76*	24*	73*	27*	65*	35*	78*	22*	45	55

Mean values (in %) (n=6) are displayed. SEM<6%
*Values of P<0.01 were considered statistically significant using one-way analysis of variance (ANOVA)
[a] Homogenate of hypoxic rabbit lung
[b] Homogenate of control rabbit lung
[c] Homogenate of control rat lung
[d] Homogenate of control rabbit kidney
[e] Homogenate of control rat kidney

(3) Reliable identification and quantitation by online and dual complementary UV spectrometric and tandem MS^2 detection (see specification in "Features of the developed CapTC-CP-LC-PDAD-ESI-MS^2 technique" in the Electronic Supplementary Material).

Profiling of EET enantiomers in rabbit and rat lungs and kidneys by one-step CapTC-CP-LC-PDAD-ESI-MS^2 analysis

Application of one-step CapTC-CP-LC-PDAD-ESI-MS^2 to homogenate from hypoxically ventilated rabbit lungs, control rabbit, and rat lungs and kidneys revealed source-specific chiral chromatographic profiles (Fig. 3; the corresponding MS^2 spectra of endogenous EETs are depicted in Electronic Supplementary Material Fig. S5) and enantiomeric ratios of endogenous *free* EETs (Table 1).

Although, as described [39], hypoxic challenge of rabbit lungs for 4 h elicited the enhanced generation of all EET regioisomers, chiral analysis exhibited unchanged enantiomeric EET ratios, except for 14,15-EET (Table 1), thus suggesting only partial stereospecific EET contribution to sustained hypoxic pulmonary vasoconstriction. This finding does not exclude enantiospecific contribution of the other EETs too to hypoxic pulmonary hypertension with vascular remodeling due to the induction of specific CYP isoenzyme expression under conditions of *prolonged* (16–24 h) or *chronic* (up to 1 week) hypoxia [43, 44].

Remarkably, assessment of the distribution of *free* EET enantiomers in control lungs and kidneys of rabbits and rats (Table 1) revealed both species- and organ-specific enantiomeric EET generation profiles. As the preferential formation of certain EET enantiomers is indicative of enzymatic rather than autooxidative generation and each CYP isoenzyme is known to display its characteristic enantiomer generation profile [23, 26], the results presented in Table 1 demonstrate both the biosynthetic origin of the EETs as well as species and organ specificity of CYP isoform expression.

Conclusions

Chiral analysis by CapTC-CP-LC nonoverlapping separation of *all* eight *underivatized* EET antipodes within *one* chromatographic run followed by online dual complementary PDA and tandem MS^2 detection enables highly sensitive, simultaneous, direct, and reliable identification and quantitation, thus providing comprehensive *and* rapid information about the enantioselective distribution of *free* endogenous EETs, typically occurring at very low concentrations, at once and with minimal effort but maximal sample throughput. Application of capillary-chiral one-step analysis to complex biological sources demonstrated its usefulness as a convenient and attractive method, which provides in a minimum of time the complete enantioselective EET generation profile at a glance without any laborious and/or time-consuming multistep procedures. Highly sensitive *and* routine "enantioprofiling" of *endogenous* EETs enabled by CapTC-CP-LC, and the use in physiological experiments of *exogenous* enantiomers obtained by the preparative version might be a prerequisite for new insights and elucidation of contradictory findings regarding EET physiology in future studies. To the best of our knowledge, these tasks cannot be accomplished by presently available methods.

Acknowledgements This work was supported by the Deutsche Forschungsgemeinschaft, Project KI 567/1-2 "Vaskuläre Funktionen Cytochrom P450-abgeleiteter Eicosanoide in der pulmonalen Strombahn"and Project GR 1081/4-1 "Synthese und Metabolismus von Eicosanoiden in biologischen Systemen".

References

1. Fitzpatrick FA, Murphy RC (1989) Pharmacol Rev 40:229–241
2. Roman RJ (2002) Physiol Rev 82(1):131–185
3. Kiss L, Schütte H, Mayer K, Grimm H, Padberg W, Seeger W, Grimminger F (2000) Am J Respir Crit Care Med 161:1917–1923
4. Kutsky P, Falck J, Weiss G, Manna S, Chacos N, Capdevila J (1983) Prostaglandins 26:13–21
5. Fang X, Moore SA, Stoll LL, Rich G, Kaduce TL, Weintraub NL, Spector AA (1998) Am J Physiol 275(6 Pt 2):H2113–2121
6. Fitzpatrick FA, Ennis MD, Baze ME, Wynalda MA, McGee JE, Liggett WF (1986) J Biol Chem 261(32):15334–15338
7. Heizer ML, McKinney JS, Ellis EF (1991) Stroke 22(11):1389–1393
8. Sun J, Sui X, Bradbury JA, Zeldin DC, Conte MS, Liao JK (2002) Circ Res 90(9):1020–1027
9. Harder DR, Campbell WB, Roman RJ (1995) J Vasc Res 32:79–92
10. Oltman CL, Weintraub NL, VanRollins M, Dellsperger KC (1998) Circ Res 83(9):932–939
11. Imig JD, Navar LG, Roman RJ, Reddy KK, Falck JR (1996) J Am Soc Nephrol 7(11):2364–2370
12. Fang X, Weintraub NL, Stoll LL, Spector AA (1999) Hypertension 34(6):1242–1246
13. Sacerdoti D, Gatta A, McGiff JC (2003) Prostaglandins Other Lipid Mediat 72(1–2):51–71
14. Zhu D, 2nd Bousamra M, Zeldin DC, Falck JR, Townsley M, Harder DR, Roman RJ, Jacobs ER (2000) Am J Physiol Lung Cell Mol Physiol 278(2):L335–343
15. Campbell WB, Gebremedhin D, Pratt PF, Harder DR (1996) Circ Res 78:415–423
16. Hecker M, Bara AT, Bauersachs J, Busse R (1994) J Physiol Lond 481:407–414
17. Fisslthaler B, Popp R, Kiss L, Potente M, Harder DR, Fleming I, Busse R (1999) Nature 401(6752):493–497
18. Fleming I, Fisslthaler B, Michaelis UR, Kiss L, Popp R, Busse R (2001) Pflugers Arch 442(4):511–518

19. Node K, Huo Y, Ruan X, Yang B, Spiecker M, Ley K, Zeldin DC, Liao JK (1999) Science 285(5431):1276–1279
20. Capdevila JH, Falck JR, Estabrook RW (1992) FASEB J 6:731–736
21. Zeldin DC, Plitman JD, Kobayashi J, Miller RF, Snapper JR, Falck JR, Szarek JL, Philpot RM, Capdevila JH (1995) J Clin Invest 95(5):2150–2160
22. Zeldin DC, Moomaw CR, Jesse N, Tomer KB, Beetham J, Hammock BD, Wu S (1996) Arch Biochem Biophys 330(1):87–96
23. Daikh BE, Lasker JM, Raucy JL, Koop DR (1994) J Pharmacol Exp Ther 271(3):1427–1433
24. Katoh T, Takahashi K, Capdevila J, Karara A, Falck JR, Jacobson HR Badr KF (1991) Am J Physiol 261(4 Pt 2):F578–F586
25. Karara A, Dishman E, Jacobson H, Falck JR, Capdevila JH (1990) FEBS Lett 268(1):227–230
26. Capdevila JH, Karara A, Waxman DJ, Martin MV, Falck JR, Guengueric FP (1990) J Biol Chem 265(19):10865–10871
27. Karara A, Dishman E, Blair I, Falck JR, Capdevila JH (1989) J Biol Chem 264(33):19822–19827
28. Zou AP, Fleming JT, Falck JR, Jacobs ER, Gebremedhin D, Harder DR, Roman RJ (1996) Am J Physiol 270:F822–832
29. Hammonds TD, Blair IA, Falck JR, Capdevila JH (1989) Anal Biochem 182(2):300–303
30. Oliw EH (1992) J Chromatogr 583(2):231–235
31. Zhang JY, Blair IA (1994) J Chromatogr B Biomed Appl 657 (1):23–29
32. Wei S, Brittin JJ, Falck JR, Anjaiah S, Nithipatikom K, Cui L, Campbell WB, Capdevila JH (2006) Anal Biochem 352:129–134
33. Kiss L, Bieniek E, Weissmann N, Schütte H, Sibelius U, Günther A, Bier J, Mayer K, Henneking K, Padberg W, Grimm H, Seeger W, Grimminger F (1998) Anal Biochem 261(1):16–28
34. Newman JW, Watanabe T, Hammock BD (2002) J Lipid Res 43 (9):1563–1578
35. Shang DY, Ikonomou MG, Macdonald RW (1999) J Chromatogr A 849:467–482
36. Charles L, Laure F, Raharivelomanana P, Bianchini J-P (2005) J Mass Spectrom 40:75–82
37. Oliw EH, Garscha U, Nilsson T, Cristea M (2006) Anal Biochem 354:111–126
38. Zelinski V, Borlak J (2005) Xenobiotica 35(8):811–823
39. Kiss L, Röder Y, Bier J, Weissmann N, Seeger W, Grimminger F (2008) Anal Bioanal Chem 390(2):697–714
40. Bylund J, Ericsson J, Oliw EH (1998) Anal Biochem 265:55–68
41. Nakamura T, Bratton DL, Murphy RC (1997) J Mass Spectrom 32:888–896
42. Bernstrom K, Kayganich K, Murphy RC (1991) Anal Biochem 198:203–211
43. Pokreisz P, Fleming I, Kiss L, Barbosa-Sicard E, Fisslthaler B, Falck JR, Hammock BD, Kim IH, Szelid Z, Vermeersch P, Gillijns H, Pellens M, Grimminger F, Zonneveld AJ, Collen D, Busse R, Janssens S (2006) Hypertension 47:762–770
44. Michaelis UR, Fisslthaler B, Barbosa-Sicard E, Falck JR, Fleming I, Busse R (2005) J Cell Sci 118:5489–5498